Published in final edited form as:
Stem Cells. 2011 March ; 29(3): 430–439. doi:10.1002/stem.599.

Ets2 regulates colonic stem cells and sensitivity to tumorigenesis

Jorge Múnera, **Grace Cecena**, **Paul Jedlicka**[**], **Miriam Wankell**, and **Robert G. Oshima**[*]
Tumor Development Program, Cancer Research Center, Sanford-Burnham Medical Research Institute, 10901 North Torrey Pines Rd, La Jolla, CA 92037

[**]Department of Pathology, University of Colorado Denver

Abstract

Ets2 has both tumor repressive and supportive functions for different types of cancer. We have investigated the role of Ets2 within intestinal epithelial cells in postnatal mouse colon development and tumorigenesis. Conditional inactivation of Ets2 within intestinal epithelial cells results in over representation of Ets2 deficient colon crypts within young and adult animals. This preferential representation is associated with an increased number of proliferative cells within the stem cell region and an increased rate of crypt fission in young mice that result in larger patches of Ets2 deficient crypts. These effects are consistent with a selective advantage of Ets2 deficient intestinal stem cells in colonizing colonic crypts and driving crypt fission. Ets2 deficient colon crypts have an increased mucosal thickness, an increased number of goblet cells and an increased density. Mice with Ets2 deficient intestinal cells develop more colon tumors in response to treatment with azoxymethane and dextran sulfate sodium. The selective population of colon crypts, the altered differentiation state and increased sensitivity to carcinogen-induced tumors all indicate that Ets2 deficiency alters colon stem cell number or behavior. Ets2 dependent, epithelial cell autonomous repression of intestinal tumors may contribute to protection from colon cancer of persons with increased dosage of chromosome 21.

Keywords

Ets2; stem cells; crypt fission; adenoma

INTRODUCTION

Colorectal cancer is one of the leading causes of cancer related death in the U.S. Approximately 150,000 cases and 50,000 deaths due to the disease occurred last year. Alterations in the Wnt signaling pathway are common causes of colorectal adenoma formation. Ets2, a member of the Ets family of transcription factors, is located on human chromosome 21 and has been identified as a Wnt target in colorectal cancer cells and intestinal stem cells [1]. Ets2 is expressed within intestinal crypts in both mice and humans

[*]Correspondence: rgoshima@burnham.org.

Author contribution
Jorge Munera: conception and design, collection and/or assembly of data, data analysis and interpretation, manuscript composition
Grace Wood: collection and/or assembly of data
Paul Jedlicka: data analysis
Miriam Wankell: collection and/or assembly of data
Robert G. Oshima: conception and design, data analysis and interpretation, manuscript composition

Disclosure of Potential Conflicts of Interest
The authors indicate no potential conflicts of interest.

[2] and may be both a direct Wnt pathway target, as revealed by T-cell factor (TCF) binding sites in the Ets2 promoter and indirectly regulated by the Achaete Scute-Like 2 transcription factor (Ascl2), a direct Wnt target in intestinal stem cells [3].

Ets2 is reported to contribute to the repression of *adenomatous polyposis coli* multiple intestinal neoplasia (APC^{min})induced, intestinal tumor formation in a mouse model of human trisomy 21 [4]. The smallest interval of trisomy that resulted in decreased intestinal tumors arising in mice carrying a mutation of the Apc tumor suppressor gene ($Apc^{min/+}$) included Ets2 among 30 candidate genes. Combining a targeted Ets2 allele with the additional chromosomal intervals revealed an Ets2 copy number dependent suppression of intestinal tumors. The authors suggested that the Ets2 tumor repressive activity might be active against multiple types of tumors and thus support the hypothesis that trisomy 21 may confer broad resistance to cancer. However, another recent study using the Tc1 transchromosomic mouse model of Down's syndrome found that human genes located on Hsa21 but not including Ets2, restricted transplanted tumor growth by limiting angiogenesis [5]. In contrast to a tumor repressive effect, we have previously shown that Ets2 has a stromal, supportive function on multiple transgenic mouse mammary tumor models [6–8].

Stem cells appear to be the cell of origin of colorectal cancer based on their existence throughout the lifetime of an individual and thus their capacity to acquire the multiple genetic mutations which lead to colorectal cancer. Direct evidence for intestinal stem cells as the source of intestinal tumors came from a study of tissue specific expression of Cre recombinases to inactivate a conditional *Apc* allele [9]. Whereas deletion of *Apc* in non-stem cells resulted in adenomas at very low frequency and with long latency, inactivation of *Apc* within stem cells led to formation of macroscopic adenomas within 36 days. Furthermore, these adenomas retained a small percentage of cells which expressed the intestinal stem cell marker Lgr5. These data support the view that intestinal stem cells are the target of the origin of intestinal cancer. Alteration of intestinal stem cell number or proliferation state may increase the probability of intestinal tumorigenesis.

Here we have tested the epithelial cell autonomous function of Ets2 during chemical carcinogenesis of the colon by using a conditional Ets2 allele and a transgene expressing Cre recombinase only in intestinal epithelial cells. We show that Ets2 deficient intestinal stem cells may have a selective advantage at colonizing colon crypts and an increased probability of colon tumor development when challenged by azoxymethane (AOM), a chemical carcinogen. We show that Ets2 has an epithelial cell autonomous, tumor repressive activity for colon tumors. The protective effect of increased copies of the equivalent of Hsa21 is likely due to multiple genes including Ets2 but may be tumor type dependent.

MATERIALS AND METHODS

Mice

Generation of the $Ets2^{A72}$ and $Ets2^{flox}$ alleles has been described previously [6, 10]. All mouse lines were introgressed into the FVB/N genetic background a minimum of 6 generations. $Ets2^{flox}$ was combined with the Villin-Cre (V-Cre) [11] and the R26R Cre reporter gene [12]. The R26R mice in a 129S3/SvImJ background was obtained from the Jackson Laboratories and introgressed into the C57Bl6 genetic background. Mice were genotyped by PCR as described previously [13]. For laser capture microdissection, 5 micron sections of colon stained for β-galactosidase and neutral red were dissected from colon tissue sections using MMICellCut tools and a CellCut Plus laser capture microdissection microscope (Molecular Machines and Industries). Captured tissue was digested with digestion buffer and used for PCR. For PCR of the $Ets2^{db2}$ allele, the db2fwd1 (CCGTGTAGCAGAGAGACAGG) and db2rev2 (GGGGGTCTCATACAGGACAG)

primers were used at a concentration of 1μM. For the $Ets2^{flox}$ allele the PshA1.a (GCCACAGCAAACCTCTTTCT) and PshA1.b (ACTTGTTGCATGGGACACAC) primers were used at a concentration of 5μm.

Tumor induction and analysis

For the colitis associated cancer regimen [14, 15], 8 week old mice were injected with 12.5 mg/kg of azoxymethane (AOM). A week later animals were subjected to 2.5% dextran sulfate sodium (DSS) in drinking water for 5 days followed by a 16 day recovery. The DSS cycle was repeated once more and then a final cycle of 2% DSS for 4 days with a recovery period of 10 days was done. Animals were sacrificed at the end of the regimen or after 10 additional weeks. Macroscopic tumors were observed under a dissection microscope while microadenomas were counted from histological sections. Grading of adenomas was performed by 2 independent pathologists blinded to genotype.

Histology

Dissected colons were prepared as described [16] and fixed with either 4% formaldehyde in PBS or 2% paraformaldehyde and 0.2% glutaraldehyde in PBS for β-galactosidase staining. β-galactosidase staining was performed over night with 1 mg/ml X-gal [17]. Fixed tissues was prepared as Swiss rolls, dehydrated, embedded, sectioned and stained with hematoxylin and eosin or with neutral red for x-gal stained material by standard methods. Slides were scanned with a 20X objective using an Aperio Scanscope XT slide scanner. Digital images of slides were examined using Aperio Imagescope software. Measurements of length were made using the pen and ruler tools. For quantitation of proliferating cell nuclear antigen (PCNA), F480 reaction and terminal apoptotic cells by the deoxynucleotidyl transferase dUTP nick end labeling (TUNEL) method, tumor areas were defined using the ellipse tool and the area of positive reaction was measured using a threshold setting specific for each antibody.

Crypt analysis

Crypts uniformly stained for β-galactosidase activity were judged at 20x magnification on at least 80 well oriented distal colon crypts per slide. To validate this method slides were scored by an independent observer blinded to the genotype of the slide. The results from the independent observer for each individual slide were within 6% (on average) of the original measurements. Crypt fission was determined by measuring the number of crypts with bisecting fissure and a single luminal opening as previously described [18]. Patch size was measured on at least 100 well oriented crypts per section. To determine crypt depth, the perpendicular distance from the submucosa surface to the luminal surface of individual crypts was measured at six different points along length of the colon. The frequency of goblet cells was measured as others have described [19]. Briefly x-gal stained colons were stained with periodic acid schiff reagent (PAS) to visualize the mucin accumulations in goblet cells. Goblet cells were measured as a percentage of total cells within a crypt. Five different fields at 200X magnification from four mice per genotype at 30 days of age were examined. For determining the total number of cells per crypt, 25–40 well oriented crypts per genotype were measured as described [20]. For crypt density measurements, the lengths of at least three areas with 10 or more well oriented crypts were measured using the pen tool in Imagescope.

Statistical analysis

Data is presented as the mean ± standard deviation unless otherwise specified. Student T-test was used to analyze differences between two groups. The one-way ANOVA test was used

when more than 2 groups were compared. Mann-Whitney test was used when comparing two groups not displaying normal distribution.

RESULTS

Ets2 deficient intestinal stem cells selectively populate colon crypts

We combined a conditional targeted allele of Ets2 designated $Ets2^{flox}$ [10], the 12.4 kb Villin-Cre (V-Cre) recombinase transgene that is expressed throughout the intestinal epithelium [11] and the Rosa26 Cre reporter gene (R26R) that expresses β-galactosidase when activated by Cre recombinase [12]. V-Cre has been used in many studies that require the intestinal epithelial specific expression of Cre recombinase from the crypt to the villus and from the duodenum through the colon. Expression of Cre leads to recombination of the $Ets2^{flox}$ allele to yield the $Ets2^{db2}$ allele (Table 1). This deletion of the exons coding for the DNA binding domain inactivates the transcription factor and causes placental insufficiency in the whole animal [10]. We confirmed that expression of the Cre reporter gene was uniform in the epithelium of the small intestine (not shown) but was mosaically expressed in the colon [11]. Expression of the β-galactosidase reporter was greater in $Ets2^{flox/flox}$, V-Cre, R26R mice than those mice with either $Ets2^{+/+}$ or $Ets2^{flox/+}$ in combination with V-Cre and R26R (Figure 1A-1C). Enzymatic assays of β-galactosidase activity of colon tissue confirmed the histochemical pattern and demonstrated elevated expression of the reporter gene in animals homozygous for $Ets2^{flox}$ alleles in all portions of the colon with a proximal to distal gradient of decreasing reporter gene activity (Figure 1D). Sections of the stained colons contained a larger number of uniformly stained crypts in mice homozygous for the Ets2 conditional allele (Figure 2A, 2B). The expression of the R26R reporter gene is dependent on Cre activity and is expected to be concordant with recombination of the $Ets2^{flox}$ allele. As all crypt cells are derived within about 7 days from the differentiating progeny of stem cells located at the base of the crypt, the uniform staining of crypts reflects recombination in the stem cells of the crypt. In addition to being expressed within the stem cells, V-Cre is expressed in the differentiated cells of the crypt resulting in sporadic labeling of cells distal to the base. However these cells are lost as the cells migrate to a luminal position and are then shed. To confirm that uniformly stained crypts represent fully recombined $Ets2^{flox}$ alleles, laser capture, micro-dissection of sections stained for β-galactosidase activity was performed followed by PCR analysis of the $Ets2^{flox}$ alleles. Figure 2C shows that uniformly blue crypts contained the Cre mediated recombined $Ets2^{db2}$ allele. By contrast unstained crypts contained, nearly exclusively, the non-recombined $Ets2^{flox}$ allele. Thus the β-galactosidase reporter is a reliable indicator of the status of the Ets2 conditional allele. Intestinal stem cells populate the bottom of crypts that form by invagination during the first 2 weeks of postnatal life in the mouse [21]. To evaluate the apparent preferential colonization of crypts by Ets2 deficient stem cells we examined mice of different ages. In the colon, extensive areas of blue crypts were found in $Ets2^{flox/flox}$; V-Cre; R26R animals of ages 15, 30, 60 and 90 days (Figure 2D). Ets2 deficient crypts were more abundant than controls at 15 days and increased rapidly during the next two weeks to represent about 70% of all crypts. The fraction of all blue crypts in control animals increased with age resulting in approximately 40% blue crypts by 90 days of age. These results suggest that Ets2 deficient stem cells have a selective advantage in competition with Ets2 competent stem cells resulting in a greater number of uniformly stained crypts.

Ets2 deficient crypts divide more rapidly

In the mouse, crypt fission increases the number of crypts during the second to third week after birth [22]. To evaluate the fission of Ets2 deficient crypts, we measured the number of bifurcating crypts at day 15 and 30. Figure 3A shows representative images of bifurcating crypts and a summary of measuring the number of dividing crypts. Crypts in division were

much more numerous at D15 than later, as expected from previous studies. Animals homozygous for the Ets2 conditional allele, in addition to the V-Cre and R26R genes, contained twice as many dividing crypts as animals heterozygous or wild type for Ets2 (Figure 3D, age 15). This difference is apparent even though only about 40% of the crypts at this age were colonized by Ets2 deficient cells (Figure 2). By 30 days of age, the number of dividing crypts greatly decreased and the number of bifurcating crypts was insufficient to distinguish the Ets2 genotypes. At 15 days the fraction of Ets2 deficient crypts in fission was found to be over 30% while only about 10–12% of similarly stained crypts from the Ets2 heterozygote or wild type were found to be dividing (Figure 3E). If increased crypt fission is a cause of expansion of the Ets2 deficient monoclonal crypts, neighboring crypts should have the same genotype and the patch size of crypts would be expected to be larger than control crypts. The patch size of Ets2 deficient crypts is larger than control mice heterozygous for $Ets2^{flox}$ for ages greater than 15 days (Figure 3F, Figure 1A). Thus even though crypt fission greatly decreases after 15 days, the results of that increased rate of fission persists in the adult animals. These results are consistent with more rapidly dividing crypts at an early age, not just a larger number of Ets2 deficient crypts. Crypt fission is increased in colons of both Apc^{min} mice and human FAP samples [23].

Ets2 deficiency results in increased proliferation at the base of colon crypts

The selective advantage of Ets2 deficient intestinal stem cells could be due to increased mitotic activity of the stem cells thus providing a greater probability of out competing neighboring Ets2 competent stem cells. To measure the proliferation status of the cells of Ets2 deficient crypts, we identified cells actively synthesizing DNA by reaction with proliferative cell nuclear antigen (PCNA) antibody and scored the location of the PCNA positive cells along the entire depth of the crypt (Figure 4). An increased number of PCNA positive cells were located in the bottom third of crypts in mice with Ets2 deficient crypts. At ages of 60–80 days approximately 70% of the colon crypts of $Ets2^{flox/flox}$, V-Cre mice are Ets2 deficient (Figure 4). These results support the view that Ets2 deficiency alters the balance between self renewal and differentiation resulting in more proliferative cells within the stem cell environment.

If Ets2 deficiency causes an alteration in the self renewal of intestinal stem cells, some difference in the differentiated state of colon crypts might be expected. While the overall histological appearance of the intestines of animals with Ets2 deficient intestinal epithelial appear normal, the thickness of the colonic mucosa of mice with Ets2 deficient crypts was greater (supplementary data, Figure S1A). This increased depth of the crypts accommodated an increased number of goblet cells/crypt (supplementary data, Figure S1B) with no change in the total number of cells/crypt (supplementary data, Figure S1C). In addition, Ets2 deficient crypts occur at a higher density than crypts which retain Ets2 (supplementary data, Figure S1D). These results suggest that Ets2 deficiency may alter the balance of self renewal and differentiation resulting in increased mitotic activity, increased number of goblet cells/crypt and increased frequency of crypt fission. However, all of these differences appear to be tolerated within the normal functional requirements of the colon.

Ets2 acts within intestinal epithelial cells to repress experimental colon adenoma formation

If Ets2 restricts the self renewal of colonic stem cells, a mitotically more active or larger number of intestinal stem cells might render Ets2 deficient intestinal epithelium more sensitive to neoplastic conversion. To determine if Ets2 may repress intestinal tumor formation in an epithelial cell autonomous way, we subjected $Ets2^{flox/flox}$, V-Cre and control mice to AOM exposure and the dextran sodium sulfate induced colitis regime that results in beta-catenin activating mutations and colon adenomas [14, 15]. Mice with Ets2 deficient

crypts developed significantly more adenomas than control animals (Figure 5B). Animals heterozygous for the conditional Ets2 allele had a tumor number that was nearly identical to $Ets2^{flox/flox}$ mice not expressing Cre. At an age of 60 days, when the mice were treated with AOM, about 70% of the colon crypts of $Ets2^{flox/flox}$, V-Cre mice are monoclonal Ets2 deficient (Figure 5B). We estimate that if all crypts of an animal were Ets2 deficient, the number of tumors/animal might be twice that of control animals (Figure 5B). While tumor number was influenced by Ets2 gene activity, tumor size and pathological state were not (Supplementary data, Table S1). Furthermore, neither PCNA immunohistochemistry nor apoptotic cell index distinguished the tumor genotype. This is consistent with Ets2 influencing the initiation of colon tumor formation.

Increased representation of Ets2 deficient tumor cells

To evaluate the representation of Ets2 deficient tumor cells, PCR analysis of dissected tumors was performed. All 17 $Ets2^{flox/flox}$, V-Cre tumors revealed both $Ets2^{flox}$ and $Ets2^{db2}$ recombined alleles but none had exclusively $Ets2^{flox/flox}$ alleles (Table 2). As non-epithelial stromal cells are commonly found within these adenomas [24], we performed laser capture microdissection and PCR to evaluate the recombined status of the epithelial cells of $Ets2^{flox/flox}$, V-Cre tumors. The epithelial cells of nine tumors contained only $Ets2^{db2}$ alleles while one contained a minor level of $Ets2^{flox}$ (Table 2). As approximately 30% of the crypts at the time of AOM treatment were $Ets2^{flox/flox}$, a similar fraction of tumors would be expected if Ets2 inactivation was neutral. The over representation of Ets2 deficient epithelial cells within adenoma tumor cells supports the view that Ets2 deficiency increases sensitivity to colon tumor initiation through an epithelial cell autonomous cellular mechanism. In contrast to tumors from V-Cre mice homozygous for the $Ets2^{flox}$ allele, five of 17 tumors from V-Cre mice heterozygous for $Ets2^{flox}$ showed no signs of recombination. This was fewer than expected but more than tumors from $Ets2^{flox/flox}$, V-Cre mice. This increased frequency of tumors with recombined $Ets2^{flox}$ alleles may reflect a modest increased sensitivity to tumor formation with modestly decreased Ets2 activity.

Ets2 regulation by MAP kinase contributes to colon tumor repression

Ets2 is activated by phosphorylation of a single threonine in the evolutionarily conserved N-terminal Pointed domain that mediates docking and phosphorylation by Erk [25, 26]. We replaced Thr-72 with an alanine in the Ets2 gene to produce a hypomorphic allele ($Ets2^{A72}$) in mice that permits survival in the homozygote state but is insufficient for placental function when combined with the knockout allele $Ets2^{db1}$ [6]. In order to determine if activation of Ets2 through Thr-72 is important for its repressive activity on AOM induced colon adenomas, we subjected $Ets2^{A72/A72}$ females to the AOM/DSS tumor induction protocol. 70% of the $Ets2^{A72/A72}$ (AA) animals developed tumors while less than 30% of the control animals had tumors (Figure 5C). The average tumor number was greater in the $Ets2^{A72/A72}$ mice (Figure 5D) although the average tumor size did not distinguish the two groups (data not shown). Histochemical analysis of PCNA, TUNEL and F4/80 in tumors also did not distinguish the experimental groups (supplementary data, Figure S2). Thus activation of Ets2 through The-72 is important for the tumor repressive activity of Ets2 and most likely affects tumor initiation.

DISCUSSION

Ets2 has different functions in different cell types and tumors. Previously we have shown that Ets2 supports mammary tumors through a stromal effect [6, 8] that was identified as fibroblasts [27]. However, in intestine an Ets2 copy-number dependent repression of Apc^{min} induced tumors was found in the DS1 region of the mouse ortholog of human chromosome 21 [4]. Recently a different region of Hsa21 that does not include Ets2 was implicated in

inhibiting tumor angiogenesis of transplantable tumors in a second mouse model of Down's syndrome [5]. Our results indicate that Ets2 acts within intestinal epithelial cells to repress chemical carcinogen induced colon tumors and this activity is likely associated with restricting intestinal stem cells. Thus Ets2 may be additive with other mouse orthologs and human genes located on Hsa21 to repress tumors. However, this Ets2 contribution may be specific to intestinal tumors driven by the Wnt pathway. Thus multiple genes of Hsa21 may contribute to resistance to cancer via different tumor specific mechanisms. A role for Ets2 within intestinal stem cells was anticipated from the identification of Ets2 as a target of the Wnt pathway [1, 28] and its regulation by Ascl2 in intestinal stem cells [3]. However, in contrast to the conditional inactivation of Wnt targets Ascl2 and Myc, inactivation of Ets2 within the intestinal epithelium leads to increased crypt cell proliferation and increased tumor sensitivity [3, 29] rather than the loss of Myc or Ascl2 deficient crypts. Ets2 acts to moderate the proliferation response of the Wnt pathway within the intestine like Lgr5, a stem cell marker and Wnt target [30]. The potential interaction of Ets2 within the Wnt pathway in altering colon stem cell fate is shown in Figure 5E.

We deduce that Ets2 regulates colonic stem cell self renewal because of the over representation of uniformly Ets2 deficient crypts. Competition between intestinal stem cells results in monoclonal crypt conversion, even between equally competitive cells [31–33]. The identification of crypts of $Ets2^{+/+}$, V-Cre and $Ets2^{flox/+}$, V-Cre that uniformly express the R26R reporter gene are examples of normal monoclonal conversion [34, 35]. The competitive advantage of Ets2 deficient stem cells may be reflected by the increased number or activity of proliferative cells at the bottoms of colon crypts. While the epithelium autonomous function of Ets2 revealed by Villin-Cre might be elicited through cells adjacent to the stem cells [33], the over representation of Ets2 deficient tumor cells within tumors suggests a tumor cell autonomous function. Direct proof of a stem cell autonomous function must necessarily await quantitation of isolated colonic stem cells in the presence and absence of active Ets2.

Stem cell colonization and crypt fission appear closely related. However, the regulation of crypt fission has not been studied extensively. APC mutations that drive adenoma formation from a stem cell, results in increased crypt fission perhaps even in the absence of increased epithelial cell proliferation [23]. The re-emergence of intestinal crypts that express Myc or Ascl2 after the conditional inactivation of either gene reveals a connection between competitive advantage of stem cells and increased crypt fission [3, 29]. Fission has been implicated as a mechanism for spread of mutations in the intestine of both mice and humans [36, 37]. To date alterations in genes that affect intestinal stem cells (APC, Myc, Ascl2), also affect crypt fission. The possible expansion of Ets2 deficient stem cells within individual crypts and by crypt fission may result in an expanded population of colonic stem cells. One consequence of a larger population of Ets2 deficient colonic stem cells number would be an expected increase in AOM induced tumor sensitivity because the intestinal stem cells are the cell of origin of intestinal tumorigenesis in mice [9]. This prediction was supported by the AOM/DSS experiments with $Ets2^{flox/flox}$, V-Cre and the $Ets2^{A72/A72}$ animals.

The activation of Ets2 through the phosphorylation of threonine 72 is important for its tumor repressive activity. This may reflect the dual roles of Ras/Erk activation in senescence of normal cells and its oncogenic role in cancer. For intestinal stem cells Ets2 may integrate the increased activity of the Wnt pathway and growth factor signaling normally associated with mitotic activity. Ets2 contributes to the regulation of multiple genes that may influence intestinal stem cell self renewal or differentiation. Cdx2 expression is decreased within the colons of Ets2 deficient mice rescued from placental insufficiency [10]. Cdx2 regulates early intestinal morphogenesis as well as early embryonic axis development [38] and suppresses

tumorigenesis in the distal colon in response to AOM injections [39]. MMP9 expression is decreased in some but not all expressing tissues of Ets2 deficient mice [13] and is important for differentiation towards the absorptive lineage. MMP-9 deficiency may lead to Notch1 inhibition and subsequent accumulation of goblet cells [40]. MMP9 also acts as a tumor suppressor in colitis associated cancer [41]. Finally Ets2 has been suggested to be important in restricting the self renewal of primary fibroblasts by regulating p16 [42]. Ets2 regulation of p16 may be restricted by degradation of Ets2 by the Cdh1 component of the anaphase promoting complex during the cell cycle [43]. Confirmation of involvement of any or all of these Ets2 targets will be most definitively evaluated in isolated Ets2 deficient colonic stem cells.

In summary our results indicate that while Ets2 is a Wnt pathway target gene within intestinal stem cells, its loss provides a competitive advantage for intestinal stem cells to colonize crypts, increase basal crypt cell proliferation and increases crypt fission. Ets2 loss may increase the number or sensitivity of colon stem cells for tumor initiation.

Supplementary Material

Refer to Web version on PubMed Central for supplementary material.

Acknowledgments

This work was supported by grants from the NIDDK and NCI (RO1 DK092084, P01 CA102583) and a pilot grant from the Cancer Center Support grant P30 CA30199. J.M was supported by a research supplement to promote diversity in health-related research P01-CA102583-05S1. We thank Robbin Newlin of the Histology Resource and Katina Candee, Michael Florio and Adriana Charbono of the Animal Facility Resource for expert technical assistance. We thank Deborah Gumucio, University of Michigan Medical School and Frank Gonzales, NIH for the Villin-Cre mice.

References Cited

1. van de Wetering M, Sancho E, Verweij C, et al. The beta-catenin/TCF-4 complex imposes a crypt progenitor phenotype on colorectal cancer cells. Cell. 2002; 111:241–250. [PubMed: 12408868]
2. Segditsas S, Sieber O, Deheragoda M, et al. Putative direct and indirect Wnt targets identified through consistent gene expression changes in APC-mutant intestinal adenomas from humans and mice. Hum Mol Genet. 2008; 17:3864–3875. [PubMed: 18782851]
3. van der Flier LG, van Gijn ME, Hatzis P, et al. Transcription factor achaete scute-like 2 controls intestinal stem cell fate. Cell. 2009; 136:903–912. [PubMed: 19269367]
4. Sussan TE, Yang A, Li F, et al. Trisomy represses Apc(Min)-mediated tumours in mouse models of Down's syndrome. Nature. 2008; 451:73–75. [PubMed: 18172498]
5. Reynolds LE, Watson AR, Baker M, et al. Tumour angiogenesis is reduced in the Tc1 mouse model of Down's syndrome. Nature. 2010; 465:813–817. [PubMed: 20535211]
6. Man AK, Young LJT, Tynan J, et al. Ets2-dependent stromal regulation of mouse mammary tumors. Mol Cell Biol. 2003; 23:8614–8625. [PubMed: 14612405]
7. Neznanov N, Man AK, Yamamoto H, et al. A single targeted Ets2 allele restricts development of mammary tumors in transgenic mice. Cancer Res. 1999; 59:4242–4246. [PubMed: 10485465]
8. Tynan JA, Wen F, Muller WJ, et al. Ets2-dependent microenvironmental support of mouse mammary tumors. Oncogene. 2005; 24:6870–6876. [PubMed: 16007139]
9. Barker N, Ridgway RA, van Es JH, et al. Crypt stem cells as the cells-of-origin of intestinal cancer. Nature. 2009; 457:608–611. [PubMed: 19092804]
10. Wen F, Tynan JA, Cecena G, et al. Ets2 is required for trophoblast stem cell self-renewal. Dev Biol. 2007; 312:284–299. [PubMed: 17977525]
11. Madison BB, Dunbar L, Qiao XT, et al. Cis elements of the villin gene control expression in restricted domains of the vertical (crypt) and horizontal (duodenum, cecum) axes of the intestine. J Biol Chem. 2002; 277:33275–33283. [PubMed: 12065599]

12. Soriano P. Generalized lacZ expression with the ROSA26 Cre reporter strain. Nat Genet. 1999; 21:70–71. [PubMed: 9916792]
13. Yamamoto H, Flannery ML, Kupriyanov S, et al. Defective trophoblast function in mice with a targeted mutation of Ets2. Genes Dev. 1998; 12:1315–1326. [PubMed: 9573048]
14. Greten FR, Eckmann L, Greten TF, et al. IKKbeta links inflammation and tumorigenesis in a mouse model of colitis-associated cancer. Cell. 2004; 118:285–296. [PubMed: 15294155]
15. Okayasu I, Ohkusa T, Kajiura K, et al. Promotion of colorectal neoplasia in experimental murine ulcerative colitis. Gut. 1996; 39:87–92. [PubMed: 8881816]
16. Neufert C, Becker C, Neurath MF. An inducible mouse model of colon carcinogenesis for the analysis of sporadic and inflammation-driven tumor progression. Nat Protoc. 2007; 2:1998–2004. [PubMed: 17703211]
17. Lobe CG, Koop KE, Kreppner W, et al. Z/AP, a double reporter for Cre-mediated recombination. Dev Biol. 1999; 208:281–292. [PubMed: 10191045]
18. Wang Y, Wang L, Iordanov H, et al. Epimorphin(−/−) mice have increased intestinal growth, decreased susceptibility to dextran sodium sulfate colitis, and impaired spermatogenesis. J Clin Invest. 2006; 116:1535–1546. [PubMed: 16710473]
19. Gregorieff A, Stange DE, Kujala P, et al. The Ets-domain transcription factor Spdef promotes maturation of Goblet and Paneth cells in the intestinal epithelium. Gastroenterology. 2009; 137:1333–1345. [PubMed: 19549527]
20. Ramsay RG, Micallef S, Lightowler S, et al. c-myb Heterozygous mice are hypersensitive to 5-fluorouracil and ionizing radiation. Mol Cancer Res. 2004; 2:354–361. [PubMed: 15235111]
21. Menard D, Dagenais P, Calvert R. Morphological changes and cellular proliferation in mouse colon during fetal and postnatal development. Anat Rec. 1994; 238:349–359. [PubMed: 8179216]
22. Cheng H, Bjerknes M. Whole population cell kinetics and postnatal development of the mouse intestinal epithelium. Anat Rec. 1985; 211:420–426. [PubMed: 3993991]
23. Wasan HS, Park HS, Liu KC, et al. APC in the regulation of intestinal crypt fission. J Pathol. 1998; 185:246–255. [PubMed: 9771477]
24. Biswas S, Chytil A, Washington K, et al. Transforming growth factor beta receptor type II inactivation promotes the establishment and progression of colon cancer. Cancer Res. 2004; 64:4687–4692. [PubMed: 15256431]
25. Wasylyk C, Bradford AP, Gutierrez-Hartmann A, et al. Conserved mechanisms of Ras regulation of evolutionary related transcription factors, Ets1 and Pointed P2. Oncogene. 1997; 14:899–913. [PubMed: 9050989]
26. Brunner D, Ducker K, Oellers N, et al. The ETS domain protein pointed-P2 is a target of MAP kinase in the sevenless signal transduction pathway. Nature. 1994; 370:386–389. [PubMed: 8047146]
27. Trimboli AJ, Cantemir-Stone CZ, Li F, et al. Pten in stromal fibroblasts suppresses mammary epithelial tumours. Nature. 2009; 461:1084–1091. [PubMed: 19847259]
28. Van der Flier LG, Sabates-Bellver J, Oving I, et al. The Intestinal Wnt/TCF Signature. Gastroenterology. 2007; 132:628–632. [PubMed: 17320548]
29. Muncan V, Sansom OJ, Tertoolen L, et al. Rapid loss of intestinal crypts upon conditional deletion of the Wnt/Tcf-4 target gene c-Myc. Mol Cell Biol. 2006; 26:8418–8426. [PubMed: 16954380]
30. Garcia MI, Ghiani M, Lefort A, et al. LGR5 deficiency deregulates Wnt signaling and leads to precocious Paneth cell differentiation in the fetal intestine. Dev Biol. 2009; 331:58–67. [PubMed: 19394326]
31. Ponder BA, Schmidt GH, Wilkinson MM, et al. Derivation of mouse intestinal crypts from single progenitor cells. Nature. 1985; 313:689–691. [PubMed: 3974703]
32. Schmidt GH, Winton DJ, Ponder BA. Development of the pattern of cell renewal in the crypt-villus unit of chimaeric mouse small intestine. Development. 1988; 103:785–790. [PubMed: 3248525]
33. Snippert HJ, van der Flier LG, Sato T, et al. Intestinal crypt homeostasis results from neutral competition between symmetrically dividing Lgr5 stem cells. Cell. 2010; 143:134–144. [PubMed: 20887898]

34. He XC, Yin T, Grindley JC, et al. PTEN-deficient intestinal stem cells initiate intestinal polyposis. Nat Genet. 2007; 39:189–198. [PubMed: 17237784]

35. Loeffler M, Bratke T, Paulus U, et al. Clonality and life cycles of intestinal crypts explained by a state dependent stochastic model of epithelial stem cell organization. J Theor Biol. 1997; 186:41–54. [PubMed: 9176636]

36. Greaves LC, Preston SL, Tadrous PJ, et al. Mitochondrial DNA mutations are established in human colonic stem cells, and mutated clones expand by crypt fission. Proc Natl Acad Sci U S A. 2006; 103:714–719. [PubMed: 16407113]

37. Park HS, Goodlad RA, Wright NA. Crypt fission in the small intestine and colon. A mechanism for the emergence of G6PD locus-mutated crypts after treatment with mutagens. Am J Pathol. 1995; 147:1416–1427. [PubMed: 7485404]

38. Tamai Y, Nakajima R, Ishikawa T, et al. Colonic hamartoma development by anomalous duplication in Cdx2 knockout mice. Cancer Res. 1999; 59:2965–2970. [PubMed: 10383162]

39. Bonhomme C, Duluc I, Martin E, et al. The Cdx2 homeobox gene has a tumour suppressor function in the distal colon in addition to a homeotic role during gut development. Gut. 2003; 52:1465–1471. [PubMed: 12970140]

40. Garg P, Ravi A, Patel NR, et al. Matrix metalloproteinase-9 regulates MUC-2 expression through its effect on goblet cell differentiation. Gastroenterology. 2007; 132:1877–1889. [PubMed: 17484881]

41. Garg P, Sarma D, Jeppsson S, et al. Matrix metalloproteinase-9 functions as a tumor suppressor in colitis-associated cancer. Cancer Res. 2010; 70:792–801. [PubMed: 20068187]

42. Ohtani N, Zebedee Z, Huot TJ, et al. Opposing effects of Ets and Id proteins on p16INK4a expression during cellular senescence. Nature. 2001; 409:1067–1070. [PubMed: 11234019]

43. Li M, Shin YH, Hou L, et al. The adaptor protein of the anaphase promoting complex Cdh1 is essential in maintaining replicative lifespan and in learning and memory. Nat Cell Biol. 2008; 10:1083–1089. [PubMed: 19160489]

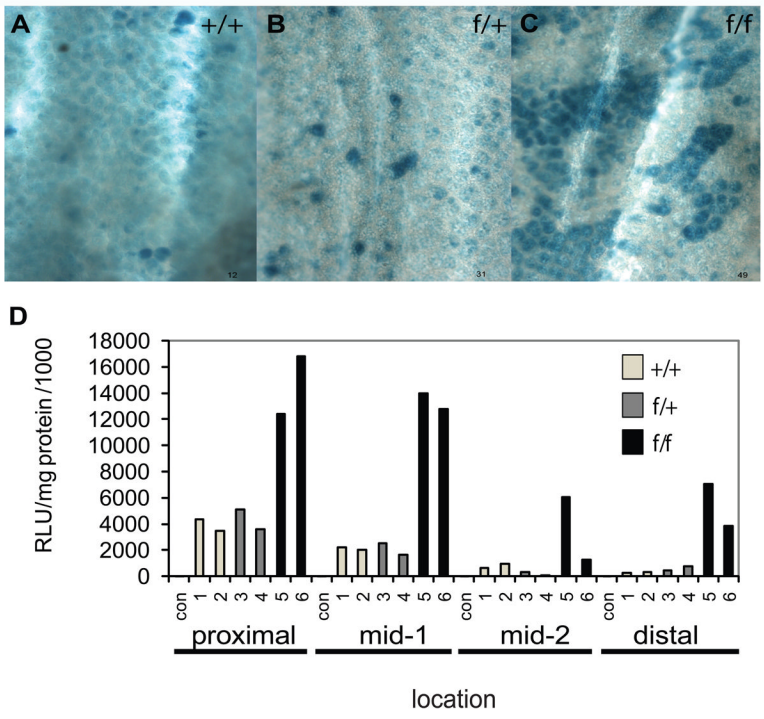

Figure 1.

Increased representation of Ets2 deficient colons crypts. Representative whole mount images of distal colon areas stained for β-galactosidase. Examples are from areas 1 cm from the anus of 15 day female mice containing V-Cre, the R26R reporter gene and : (**A**) $Ets2^{+/+}$; (**B**) $Ets2^{flox/+}$; (**C**) $Ets2^{flox/flox}$ alleles. Note larger patches of blue stained crypts in $Ets2^{flox/flox}$ genotype. (**D**) Ets2 dependence of β-galactosidase activity of the colon. The colons of 18 day old mice were divided into four portions (proximal, mid-1, mid-2 and distal) homogenized and enzyme activity and protein content was determined. Two animals each of R26R, V-Cre mice with wt $Ets2^{+/+}$, open bars, 1–2; $Ets2^{flox/+}$, gray bars, 3–4; or $Ets2^{flox/flox}$, black bars, 5–6, were compared.

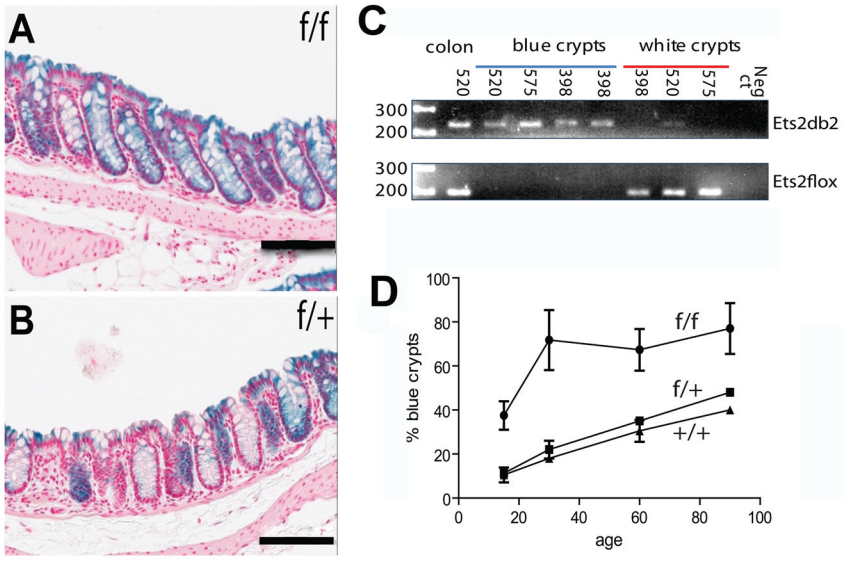

Figure 2.

Ets2 dependence of uniformly populated crypts. (A) representative sections of colon from Ets2 $^{flox/flox}$, V-Cre, R26R; (**B**) Ets2$^{flox/+}$, V-Cre, R26R mice stained for β-galactosidase (blue) and with neutral red. Black bars represent 100 microns. (**C**) agarose gel analyses of PCR products of approximately 10 pooled individual crypt sections recovered by laser capture microdissection of β-galactosidase positive and negative crypts from Ets2$^{flox/flox}$, V-Cre, R26R mice. Mouse number from which the sections were obtained is indicated at the top. Ets2 genotype is indicated at right. Size marker are at left in bp. The “colon” sample represents whole tissue control. Ets2^{flox} is recombined by Cre to generate the Ets2^{db2} allele in β-galactosidase positive crypts. (**D**) frequency of uniformly blue crypts was measured in sections of animals of different ages. The values represent the averages of at least 85 scored crypts from two sections of at least two mice of each genotype and age except for Ets2$^{+/+}$ at 30 days and Ets2$^{flox/+}$ at 90 days for which only one mouse was available. Two tailed Student t-test indicated the results for mice with the Ets2$^{flox/flox}$ genotype was significantly different from Ets2$^{flox/+}$ or Ets2$^{+/+}$.

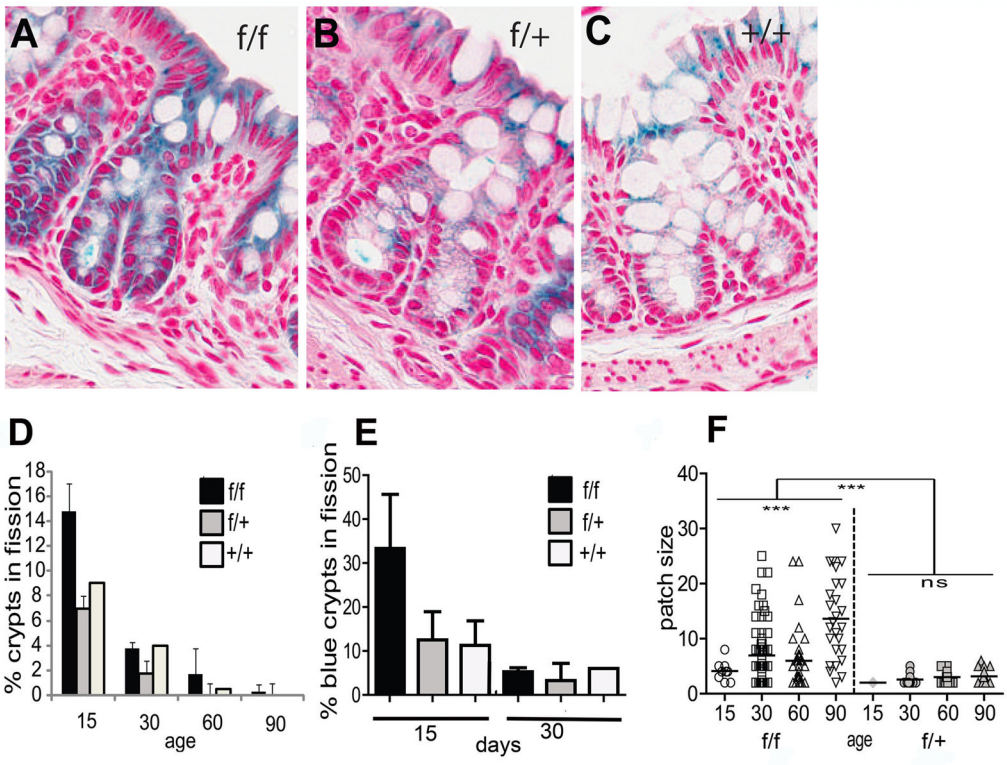

Figure 3.

Crypt fission is increased in Ets2 deficient colons. Sections of V-Cre, R26R mice of varying Ets2 genotype and age stained for β-galactosidase were scored for bifurcating crypts. (**A-C**) examples of crypts in fission for each genotype at postnatal day 15 (P15). (**D**) frequency of dividing crypts as a function of age. For each measurement, at least 86 well oriented crypts were scored. Error bars represent the standard deviation. The numbers of mice analyzed are the same as for Figure 2. (**E**) increased fission of Ets2 deficient crypts. Only blue crypts were scored at 15 and 30 days. F, crypt patch size increases with age in $Ets2^{flox/flox}$ but not in $Ets2^{flox/+}$ mice. Patches of two or more adjacent crypts were measured. In $Ets2^{flox/flox}$ mice, patch sizes is greater after 15 day. Patch size of $Ets2^{flox/+}$. Patch size differences within each genotype were measured using a one-way ANOVA test. For $Ets2^{flox/flox}$ mice there was a significant difference in patch sizes within the group ($p<0.0001$). Patch size in $Ets2^{flox/+}$ mice was not significantly different with age as revealed by a one-way ANOVA test ($p=0.25$). ns = not significant. Differences in patch size between the two genotypes was determined by Mann-Whitney test ($p<0.0001$).

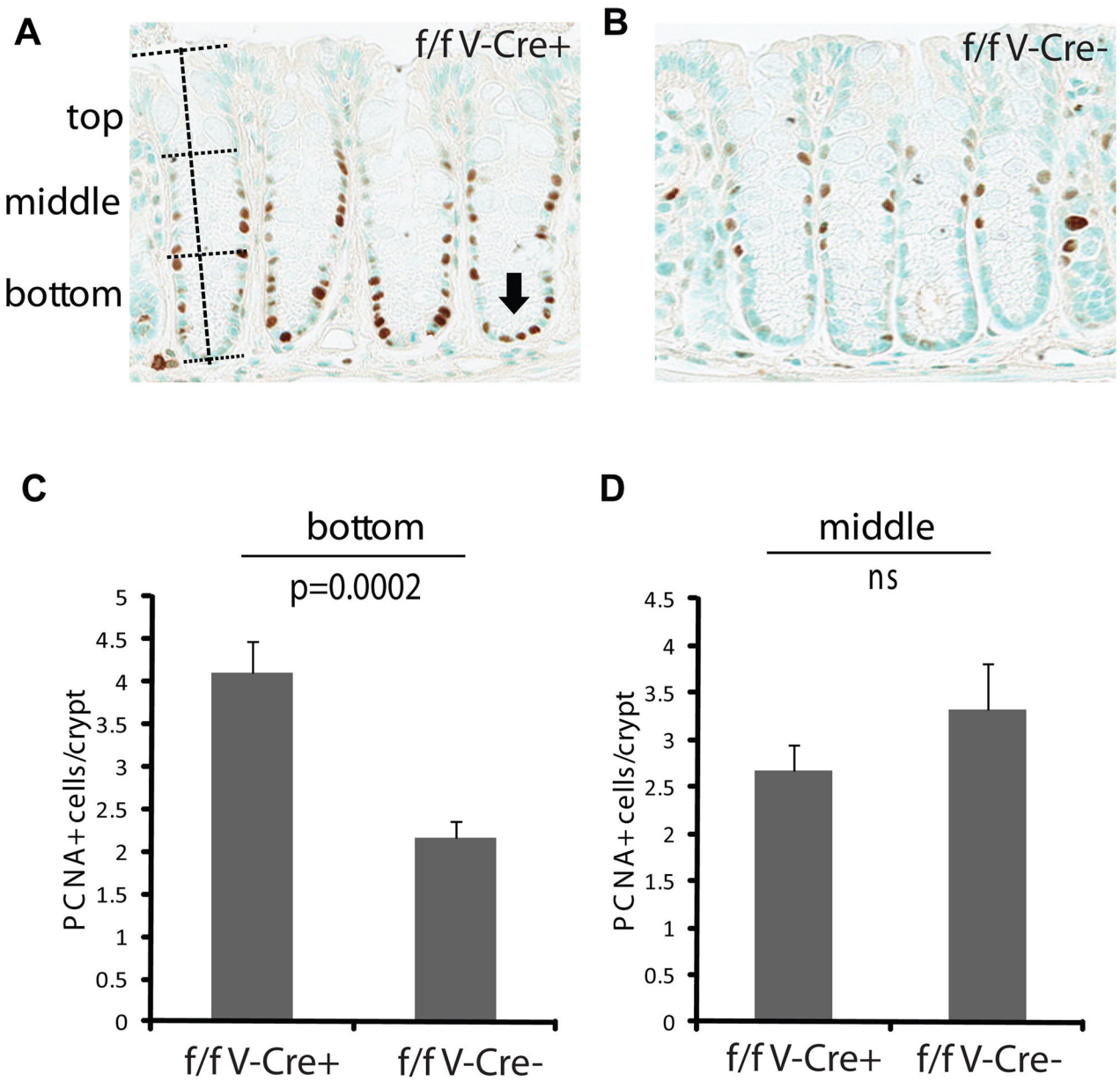

Figure 4.

Increased proliferation at the bottom of crypts from Ets2 deficient mice. (**A**) DAB reaction (brown) indicates reaction of nuclei with antibody to PCNA. The height of individual crypts (vertical dotted line) was measured and used to divide the crypt into thirds (horizontal dotted lines). The arrow indicated PCNA positive cells in the bottom of crypts from $Ets2^{flox/flox}$ V-Cre (f/f V-Cre+) mice that are not as common in (**B**) $Ets2^{flox/flox}$ mice without V-Cre (f/f V-Cre−). (**C**) frequency of PCNA positive cells in the bottom third of colon crypt. Error bar indicates the standard deviation. (**D**) the number of PCNA positive cells in the middle third of colon crypts is not significantly different between the two genotypes.

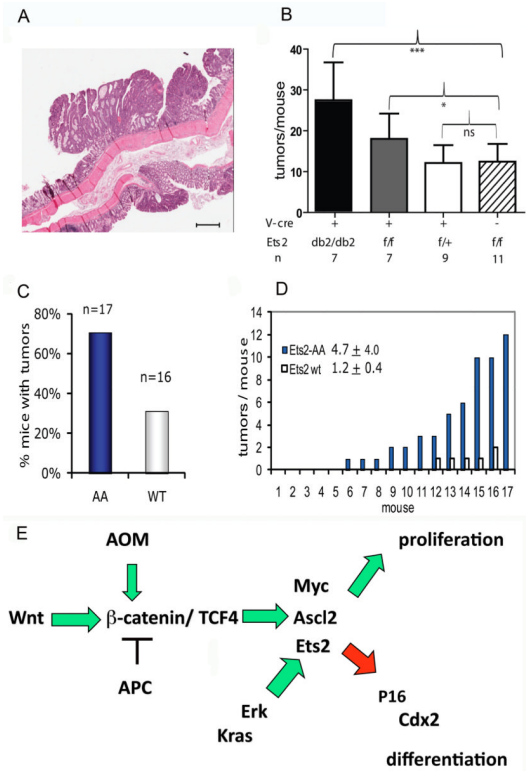

Figure 5.

Adenoma formation in mice treated with azoxymethane and dextra sodium sulfate. Multiplicity but not size is increased in $Ets2^{flox/flox}$, V-Cre mice compared to $Ets2^{flox/+}$ V-Cre and $Ets2^{flox/flox}$ mice following the 9 week AOM/DSS regimen. (**A**) Representive hematoxylin and eosin stained section of colon tumors from an $Ets2^{flox/flox}$ V-Cre, scale bar = 500 microns. (**B**) Comparison of average number of tumors per mouse from AOM/DSS treated mice of the $Ets2^{flox/flox}$, V-Cre, $Ets2^{flox/+}$, V-Creand $Ets2^{flox/flox}$ genotypes. The solid black column labeled db2/db2 represents the $Ets2^{flox/flox}$, V-Cre group adusted for the 30% of the crypts that do not express Cre at the age of AOM administration (Figure 2). N represents number of mice examined. Results of student T-test: * indicates $P < 0.05$, *** indicate P=0.001, ns, not significant. (**C**) increased sensitivity of $Ets2^{A72/A72}$ mice to AOM/DSS induced tumors. Mice were examined 19 weeks after AOM/DSS administration. (**D**) tumor number of individual mice. Each of the mice is ranked by the number of tumors found. (**E**) Schematic diagram of possible relationships of Ets2 and Wnt signaling pathway components. Ets2 may be both a direct target of β-catenin/TCF4 and downstream of Ascl2. Activation of Ets2 by Ras occurs though phosphorylation of Thr72 by Erk. P16 has been suggested to be a target of Ets2 in primary cells. Cdx2 is a direct target of Ets2 in trophoblast cells and is decreased in Ets2 deficient mouse colon.

Table 1

Summary of Gene Combinations

Alleles	Abbrev.	Description	Use	Ref.
$Ets2^{db1}$		Ets2 loss of function allele. Deletion of DNA binding domain.	Inactive Ets2	13
$Ets2^{flox}$	$Ets2^{f}$	Ets2 gene with loxP sequences flanking exons 9 and 10.	Conditional Ets2	10
$Ets2^{db2}$		Ets2 gene deletion of exons 9 and 10 caused by action of Cre recombinase on $Ets2^{flox}$.	Inactive Ets2	10
$Ets2^{T72A}$	$Ets2^{A72}$	Ets2 gene containing a targeted mutation of codon 72 converting Thr to Ala. This created a hypomorphic allele that cannot be activated by phosphorylation of Thr72.	Hypomorphic allele	6
Villin-Cre	V-Cre	A transgene containing the coding domain of Cre recombinase, driven by a 12.4 kb fragment of the mouse villin 1 gene, Cre is expressed within intestinal epithelial cells.	Recombination of Ets2 flox allele	11
Rosa26 reporter	R26R	A targeted mutation of the Rosa26locus containing a splice acceptor, a Neo expression cassette flanked by loxP sites and a LacZ gene. Cre recombinase removes the Neo cassette resulting in expression of the LacZ gene.	Identification of cells that have expressed Cre.	12
$Ets2^{flox/flox}$, Villin- Cre, R26R	$Ets2^{f/f}$ V-Cre R26R	VillinCre expression will convert the $Ets2^{flox/flox}$ alleles to $Ets2^{db2/db2}$ and activate the R26R gene to express β-galactosidase from the LacZ gene. In absence of Cre expression, cells will remain beta-galactosidase negative.	Crypt colonization, crypt fission, AOM DSS tumorigenesis and morphometric analysis.	
$Ets2^{flox/+}$, Villin-Cre, R26R	$Ets2^{f/+}$ V-Cre R26R	VillinCre expression converts the $Ets2^{flox}$ allele to $Ets2^{db2/db2}$ and activate the R26R gene to express β-galactosidase from the LacZ gene.	Crypt colonization, crypt fission, AOM DSS tumorigenesis and morphometric analysis.	
$Ets2^{+/+}$, Villin-Cre, R26R	$Ets2^{+/+}$ V-Cre R26R	VillinCre expression will activate the R26R gene to express β-galactosidase from the LacZ gene but not affect Ets2 activity.	Crypt colonization, crypt fission, AOM DSS tumorigenesis and morphometric analysis.	
$Ets2^{flox/flox}$, Villin-Cre	$Ets2^{f/f}$ V-Cre	same as above except no reporter gene is included.	AOM DSS tumor, PCNA	
$Ets2^{flox/+}$, Villin-Cre	$Ets2^{f/+}$ V-Cre	same as above except includes one wt Ets2 allele.	AOM DSS tumor	
$Ets2^{flox/flox}$	$Ets2^{f/f}$	homozygous for $Ets2^{flox}$	AOM DSS tumor, PCNA	
$Ets2^{A72/A72}$	$Ets2^{A72/A72}$	homozygous Ets2 hypomorphic alleles	AOM DSS tumors	

Table 2

Ets2 alleles within tumors

Mouse genotype	Tumor number	$Ets2^{db2}$ allele detected	$Ets2^{flox}$ allele detected	$Ets2^{flox/flox}$ or $Ets2^{flox/+}$ tumors	Expected $Ets2^{flox/flox}$ or $Ets2^{flox/+}$ tumors	Method	P value Chi- square (expected vs. observed)
$Ets2^{f/f}$ V-Cre R26R	17	17	0	0	5.1	PCR	0.0023
$Ets2^{f/f}$ V-Cre	9	9	1*	0	2.7	LCM PCR	0.035
$Ets2^{f/+}$ V-Cre	17	12	17	5	11	PCR	0.0023
$Ets2^{f/f}$	5	0	5	5	5	PCR	NS

based on fraction of recombined crypts at time of AOM treatment (Figure 2).

* detectable, but less than 25% of $Ets2^{db2}$ allele